Jpn. J. Pharmacol. **85**, 124 – 132 (2001)

Nitrooxy Alkyl Apovincaminate Activates K^+ Currents in Rat Neocortical Neurons

Mitsutoshi Munakata[1], Kazuo Noguchi[1,2,]*, Hiroaki Araki[3] and Norio Akaike[1]

[1]*Department of Cellular and System Physiology, Graduate School of Medical Sciences, Kyushu University, 1-2-2 Maidashi, Higashi-ku, Fukuoka 812-8582, Japan*
[2]*Pharmacology Laboratory, Pharmaceutical Research Laboratories, Taisho Pharmaceutical Co., Ltd., 1-403 Yoshino-cho, Ohmiya, Saitama 330-8530, Japan*
[3]*Department of Hospital Pharmacy, Okayama University Medical School, 2-5-1 Shikata-cho, Okayama 700-8558, Japan*

Received May 1, 2000 Accepted November 2, 2000

ABSTRACT—The effects of nitrooxy alkyl apovincaminate VA-045 ((+)-eburunamenine-14-carboxylic acid(2-nitroxy-ethyl ester), VA) were investigated in acutely dissociated rat neocortical neurons by using a nystatin-perforated patch recording configuration. VA activated a steady-state outward current in a concentration-dependent manner, with an EC_{50} of 0.65 μM. The reversal potential for the current shifted 56.5 mV with tenfold changes in the extracellular K^+ concentration, suggesting that the current was carried by K^+. The VA-induced current was not suppressed by apamin (1 μM), charybdotoxin (1 μM), Cs^+ (3 mM), Ba^{2+} (3 mM), 4-aminopyridine (10 mM) or glibenclamide (10 μM), whereas tetraethylammonium suppressed the current with an IC_{50} of 1.4 mM. These pharmacological properties of the VA-induced current were compatible with a slowly inactivating delayed rectifier current (I_K). It was suggested that the current activated by VA was I_K. The VA-induced current was not affected by Ca^{2+} depletion or by staurosporine (0.1 μM), quinacrine (10 μM), wortmanin (1 μM) or genistein (1 μM). The intracellular perfusion of GDPβS (0.4 mM) also had no significant effect. Thus, VA may directly activate the K^+ channels.

Keywords: VA-045, Nitrooxy alkyl apovincaminate, K^+ channel, Delayed rectifier, Neocortical neuron (rat)

Two major types of voltage-gated K^+ currents have been recognized in neurons, namely a rapidly inactivating transient current (I_A) and slowly inactivating delayed rectifier current (I_K) (1). Both channels play pivotal roles in virtually every aspect of neuronal signaling (1). Therefore, selective modulators of each current could be useful tools for understanding the physiological functions of the currents, and they might have therapeutic potential. *N*-Bromoacetamide (2) and chloramine-T (3) are known to affect the rapid inactivation of I_A, whereas no specific modulator for I_K has yet been identified.

Recently, VA-045 ((+)-eburunamenine-14-carboxylic acid(2-nitroxy-ethyl ester), VA), a novel apovincaminic acid derivative (Fig. 1) (4), has been shown to exert neuroprotective effects that ameliorate disturbances in such brain functions as memory and consciousness in a head injury model of the rat in vivo (5, 6), although the mechanism of these actions remains unknown. In the present study, we investigated the effects of VA on rat neocortical neurons to elucidate the cellular basis of the effect of VA and

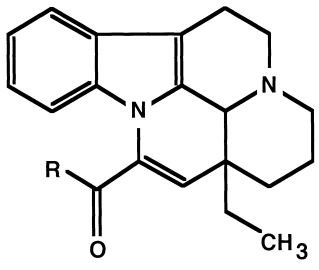

R: -$OCH_2CH_2ONO_2$ (VA-045)
: -OCH_2CH_2OH (VA-072)
: -OH (Apovincaminic acid)
: -OCH_2CH_3 (Vinpocetine)

Fig. 1. The chemical structure of nitrooxy alkyl apovincaminate VA-045 ((+)-eburunamenine-14-carboxylic acid(2-nitroxy-ethyl ester)) and related compounds.

*Corresponding author (affiliation #2). FAX: +81-48-654-6650
E-mail: s15922@ccm.taisho.co.jp

found that VA activates a specific K^+ current, presumably I_K. This cellular effect of VA may underlie the beneficial in vivo effects of the compound.

MATERIALS AND METHODS

Preparations

Single pyramidal neurons of the cerebral cortex were acutely dissociated using a method reported previously (7). Briefly, 2-week-old Wistar-strain rats were decapitated under deep ether anesthesia. The area between 2 and 4 mm from the anterior tip of the frontal lobe was then cut into coronal slices (350-μm-thick) with a microslicer (DTK-1000; Dosaka EM Co., Ltd., Kyoto) and pre-incubated in an incubation solution saturated with 95% O_2 – 5% CO_2 for 40 min at room temperature (22 – 25°C). Then, the slices were treated with enzymes in an oxygenated standard external solution for 15 min at 31°C; they were first treated with 0.015% pronase and then with 0.015% thermolysin. The dorsomedial portion of the frontal cortex was micro-punched out and dissociated mechanically with fine fire-polished glass Pasteur pipettes in a small plastic culture dish (3801; Falcon, Tokyo) filled with standard solution. The dissociated neurons adhered to the bottom of the dish within 30 min, allowing us to carry out electrophysiological studies.

Electrical measurements

Nystatin-perforated patch electrical recording (8) was performed with some modification (9). Patch pipettes were fabricated from glass capillaries (G-1.5; Narishige, Tokyo) on a two-stage puller (PB-7, Narishige). The resistance between the patch-pipette filled with internal solution and the reference electrode was 4 to 6 MΩ. After the formation of a stable perforated patch, the series resistance ranged from 14 to 18 MΩ. For conventional whole-cell recording (10, 11), in which the membrane patch was ruptured, pipettes with a resistance of 3 to 4 MΩ were used. The ionic current and membrane potential were measured with a patch-clamp amplifier (EPC-7; HEKA Electronics, Lambrecht/Pfalz, Germany). The signals were filtered with a low-pass filter (FV-665; NF Electronic Instruments, Tokyo) at a cut-off frequency of 1 kHz and were monitored simultaneously on a storage oscilloscope (MS-5100; Iwatsu, Tokyo) and a pen-recorder (RECTI HORIZ 8K; NEC San-ei, Tokyo). The signals were stored on a video-cassette recording system (HV-F93; Mitsubishi, Tokyo) via a pulse coded modulation processor (PCM 501; Sony, Tokyo) for subsequent analysis using the pCLAMP system (Axon Instruments, Inc., Foster City, CA, USA). All experiments were performed at room temperature (24 – 26°C).

Measurement of extracellular K^+ activities

The extracellular K^+ activities ($a[K^+]_o$) were estimated by using a K^+ electrode connected to an ION 85 ion analyzer (Radiometter A/S, Copenhagen, Denmark).

Solutions and their application

The ionic composition of the standard external solution was 150 mM NaCl, 5 mM KCl, 1 mM $MgCl_2$, 2 mM $CaCl_2$, 10 mM *N*-2-hydroxyethyl-piperazine-*N*′-2-ethanesulfonic acid (HEPES) and 10 mM glucose. The pH was adjusted to 7.4 with Tris (hydroxy-methyl) aminomethane base (Tris-base). The ionic composition of the incubation medium was 125 mM NaCl, 5 mM KCl, 1.2 mM KH_2PO_4, 1.3 mM $MgSO_4$, 2.4 mM $CaCl_2$, 26 mM $NaHCO_3$ and 10 mM glucose. This was aerated with 95% O_2 – 5% CO_2 gas to a final pH of 7.4. The test solution used to measure the slowly inactivated transient outward current consisted of 140 mM NaCl, 5 mM KCl, 1 mM CsCl, 1 mM $MgCl_2$, 2 mM $CaCl_2$, 3 mM $BaCl_2$, 10 mM 4-amynopyridine (4-AP), 0.001 mM tetrodotoxin (TTX), 0.0003 mM $LaCl_3$, 10 mM glucose and 10 mM HEPES (pH 7.2) (see Results). The pipette solution contained 150 mM KCl and 10 mM HEPES. The pH was adjusted to 7.2 with Tris-base. A fresh stock solution of 10 mg/ml nystatin in methanol was prepared every day and kept at –20°C. This solution was then dissolved in the pipette solution to produce a final nystatin concentration of 200 μg/ml. The pipette solution for the conventional whole-cell method contained 50 mM KCl, 70 mM K-gluconate, 20 mM NaCl, 0.25 mM $CaCl_2$, 6 mM $MgCl_2$, 5 mM Na_2ATP, 5 mM EGTA, 10 mM HEPES and 0.4 mM GTP or guanosine 5'-*o*-(2-thiodiphasphate) (GDPβS) (pH 7.2).

All drugs were applied using a rapid application system called the Y-tube method, described elsewhere (12). Using this technique, the solution surrounding a dissociated neuron could be completely exchanged within 30 ms.

Drugs

VA, VA-072, apovincaminic acid (AVA) and vinpocetine (Fig. 1) were synthesized by the Taisho Pharmaceutical Co., Ltd. (4). VA, VA-072 and vinpocetine were first dissolved in dimethylsulfoxide at a concentration of 1 mM, while 1 mM AVA was titrated to pH 7.0 using Tris-base in distilled water. These solutions were then diluted to the final concentration in the external solution. The other drugs used in this study were quinacrine, wortmanin, genistein, GDPβS, glibenclamide, thapsigargin, acetylcholine (ACh) and sodium nitroprusside (Sigma, St. Louis, MO, USA); apamin and charybdotoxin (ChTX) (Peptide Institute Inc., Tokyo); tetraethylammonium (TEA), 4-AP (Tokyo Kasei, Tokyo); ryanodine (Wako Pure Chemical Co., Tokyo); staurosporine (Kyowa Co., Tokyo); and NOR3 (Dojindo, Kumamoto).

Statistical analyses

The data are presented as the mean ± S.E.M. in the text, and a vertical bar indicates the S.E.M. in the figures.

The continuous theoretical curves for the concentration-response relationships were constructed using a modified Michaelis-Menten equation 1 with a least-squares fitting routine:

$$I = I_{max} C^n / (C^n + EC_{50}{}^n) \quad \text{Eq. 1}$$

where I represents the drug-induced current amplitude, I_{max} is the maximum value of current and C is the corresponding drug concentration. EC_{50} and n denote the half-maximum concentration and Hill slope, respectively. The equation for the concentration-inhibition curve is the mirror image of the Michaelis-Menten equation:

$$I / I_{max} = 1 - C^n / (C^n + IC_{50}{}^n) \quad \text{Eq. 2}$$

where I is the current amplitude normalized by that of the control and IC_{50} denotes the half-inhibition concentration of the antagonists.

RESULTS

The effect of VA on cortical neurons

Whole-cell recordings were made using neurons freshly dissociated from the rat neocortex, using the nystatin-perforated patch recording configuration. Figure 2Aa shows the effect of VA under the current-clamp conditions. The external application of 3×10^{-6} M VA reversibly hyperpolarized the membrane potential (Control: 57.9 ± 4.6 mV; +VA: 72.6 ± 6.2 mV (n = 6)). This effect was observed in 86% neurons tested. Then, voltage-clamp experiments were done to further analyze the hyperpolarizing effect of VA.

As shown in Fig. 2Ab, 3×10^{-6} M VA elicited a steady-state outward current (127.8 ± 7.9 pA, n = 44) at a holding potential (V_H) of –40 mV. To examine whether this current activation was related to the specific molecular structure of VA, the effects of all available related compounds (Fig. 1) were also tested. Hyperpolarizing step pulses of 10 mV, 350 ms in duration were added every 4 s to monitor the change in membrane conductance. Here, VA evoked an outward current accompanied by the membrane conductance increase, while AVA and VA-072, a denitrated metabolite of VA, did not evoke any detectable currents. Vinpocetine elicited a small outward current with an increased membrane conductance. However, the reversal potential for this compound (–35.8 ± 8.2 mV, n = 3) was different from that for VA (Fig. 4B). Therefore, vinpocetine and VA affected different ionic currents. Nitroprusside (10^{-5} M, Fig. 2B) and NOR3 (10^{-4} M, data not shown), which produces nitrooxygen, also elicited no significant responses, suggesting that the effect of VA did not result from nitrooxygen, which might be released from VA. Taken together, the effect of VA appeared to be a structure-specific effect of this compound.

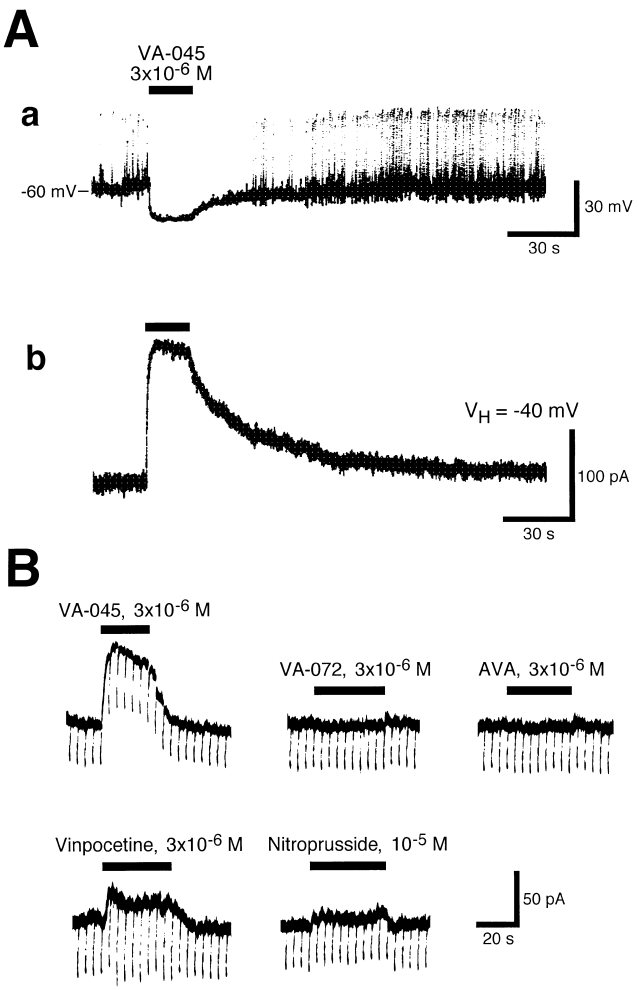

Fig. 2. The effect of VA-045 (VA) on dissociated rat neocortical neurons. Aa: The representative VA-induced response under current-clamp conditions. VA (3×10^{-6} M) was applied during the period showed by the filled horizontal bar. The peaks of the action potentials are truncated due to the narrow frequency range of the recorder. Ab: VA-induced current under voltage-clamp conditions. The holding potential (V_H) was –40 mV. The data were obtained from the same neuron used in panel a. B: The effects of compounds related to VA. To monitor the change in the membrane conductance, hyperpolarizing step pulses of 10 mV with duration of 350 ms every 4 s were continuously applied. V_H was –40 mV. All traces were obtained from the same neuron.

The concentration dependence of the effect of VA

The amplitude of the VA-induced current increased in a concentration-dependent manner. At VA concentrations higher than 3×10^{-6} M, the VA-induced current was slightly suppressed during the application of VA (open circle), resulting in an outward hump immediately after the removal of VA (solid circle) (Fig. 3A). However, dimethylsulfoxide (vehicle) up to 1% did not affect currents under the voltage-clamp condition. The cause of this transient

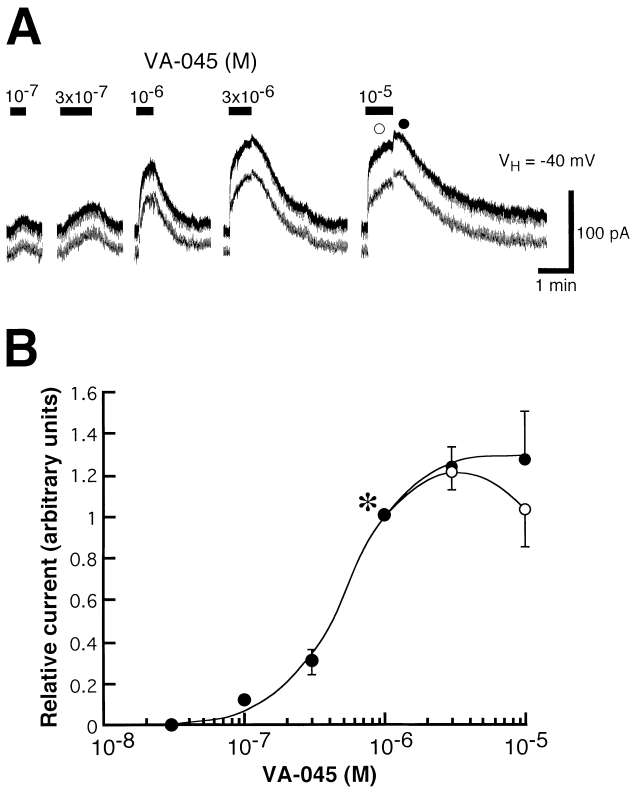

Fig. 3. The concentration-response relationship for the VA-045 (VA) effects. A: The current responses induced by different concentrations of VA. VA induced an outward current in a concentration-dependent manner. At concentrations higher than 3×10^{-6} M, the VA-induced current was slightly suppressed by VA itself (open circle), thus resulting in an outward 'hump' current just after the VA was washed out (solid circle). To monitor the change in the membrane conductance, hyperpolarizing step pulses of 10 mV with duration of 350 ms every 2 s were continuously applied. V_H was –40 mV. All traces were obtained from the same neuron. B: The concentration-response curves for the VA-induced current. The solid and open circles correspond to those in panel A. The amplitude of the current was normalized to that of the current evoked by 10^{-6} M VA (see symbol marked with an asterisk). Each point corresponds to the mean data for six neurons. Vertical bars show the S.E.M. (n = 6).

suppression of the VA-induced current remains unknown, as our study focused on the VA-induced current itself. Figure 3B summarizes the concentration-response relationship for VA. When the hump current amplitude was plotted at 10^{-5} M, the concentration-response relationship showed a close fit based on Eq. 1, with an EC_{50} and Hill coefficient of 0.65 μM and 1.6, respectively (n = 6).

The current-voltage relationships for the VA response

The VA-induced currents at various V_H's are shown in Fig. 4A. Figure 4B summarizes the I-V relationship for the VA-response. The VA response increased as the membrane depolarized to 40 mV and reversed the current direction near −82 mV. The ionic base of the VA-induced current was further investigated using the ramp-clamp method (13). TTX (1 μM), $LaCl_3$ (0.3 μM) or CsCl (1 mM) was added to the external solution to block the voltage-dependent Na^+ current, Ca^{2+} current and anomalous rectifying K^+ current, respectively. TTX, $LaCl_3$ and CsCl did not have any effect on the VA-induced current. Under these conditions, a voltage ramp of 4-s duration from −40 to −110 mV was applied both before (current 1) and during (current 2) the application of VA (Fig. 4C, inset). The descending limbs of the actual I-V plots are shown in Fig. 4C. The patch-pipette and external solutions contained 150 and 5 mM K^+, respectively. The measured reversal potential (E_{rev}) was −81.6 ± 1.6 mV (n = 4), which was close to the K^+ equilibrium potential calculated from the Nernst equation. As shown in Fig. 4D, the E_{rev} became positive as $a[K^+]_o$ increased. The plot of E_{rev} against $a[K^+]_o$ showed a close linear fit, and the slope for a tenfold change of $a[K^+]_o$ was 56.5 mV, which is close to the value calculated by the Nernst equation. Therefore, the VA-induced current was carried by K^+.

The effects of K^+ channel blockers on the VA response

Figure 5 summarizes the effects of the external application of TEA and various K^+ channel blockers on the 3×10^{-6} M VA-induced current. The current was resistant to high concentrations of Ba^{2+} (3 mM), Cs^+ (3 mM) and 4-AP (10 mM). Apamin and ChTX, both Ca^{2+}-activated K^+ channel blockers, had no effect. Glibenclamide, an ATP-sensitive K^+ channel blocker, was also ineffective. TEA strongly suppressed the VA-induced current in a concentration-dependent manner with an IC_{50} of 1.4 mM. In addition, we previously reported that when 150 mM CsCl replaced KCl in the pipette solution, the VA-induced current was also completely blocked (14).

The involvement of the delayed rectifier K^+ current in the VA response

Based on the pharmacological properties of the VA-induced current (Fig. 5), all other known conductances were blocked by the addition of 10 mM 4-AP, 3 mM $BaCl_2$, 1 mM CsCl, 1 μM TTX and 0.3 μM $LaCl_3$ to the external solution. V_H was changed from –40 to –20 mV to obtain a relatively large K^+ current amplitude. Under these conditions, a slowly inactivating transient outward current, which was considered to be I_K, was activated after a hyperpolarizing step pulse from –20 to –120 mV of 1-s duration (Fig. 6Aa1). The I_K decreased as the VA-induced current developed in a VA concentration-dependent manner. Figure 6Ab shows the effect of VA on the slow outward current with a magnified time scale. Without VA, the activation and inactivation phases of the slow outward current showed good fit to single exponential functions with respective time constants of 30.3 ± 7.1 ms (n = 7) and 2.8 ± 0.5 s (n = 7). In the presence of VA (3×10^{-6} M), the

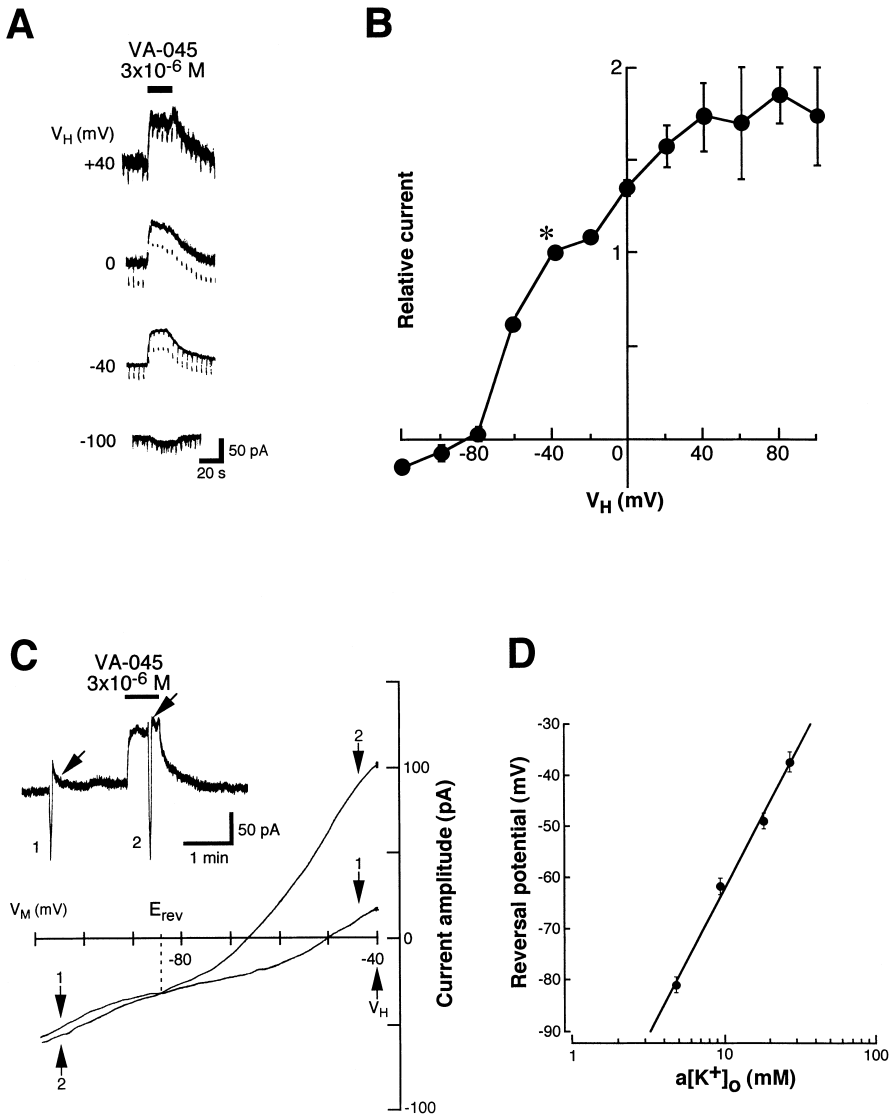

Fig. 4. The current-voltage (I-V) relationships for the VA-045 (VA)-induced current. A: The currents induced by 3×10^{-6} M VA at various V_H's. To monitor the change in the membrane conductance, hyperpolarizing step pulses of 10 mV with duration of 350 ms every 5 s were continuously applied. B: The steady state I-V relationship for the VA-induced current. The amplitude of the current was normalized to that of the current evoked at a V_H of –40 mV (see symbol marked with an asterisk). C: The I-V plots obtained by the ramp-clamp method. V_H was –40 mV, and hyperpolarizing ramp commands changing from –40 to –120 mV of 4-s duration were given before (see inset, 1) and during the application of 3×10^{-6} M VA (see inset, 2). The traces for inward-going commands are shown. V_M: membrane potential. E_{rev}: reversal potential. D: The E_{rev} for the current induced by 3×10^{-6} M VA was plotted against the extracellular K^+ activity ($a[K^+]_o$). Each point corresponds to the mean data for four neurons. Vertical bars show the S.E.M. (n = 4).

activation phase was closely correlated with the double exponential function. Initially, the outward current was activated with a time constant of 27.6 ± 5.0 ms (n = 7), which was not significantly different from that before the application of VA. However, the current then increased, with a long time constant of 1.3 ± 0.2 s (n = 7), instead of being inactivated. Figure 6B shows the effect of VA on the slow transient outward current activated at several potentials. At each potential, VA apparently removed the inactivation.

Involvement of second messenger systems

As shown in Fig. 7Aa, VA repeatedly activated outward currents in the Ca^{2+}-free external solution, suggesting that neither extracellular Ca^{2+} nor Ca^{2+} influx from the external solution were involved in the effect of VA. In addition, the VA-induced current did not change when the Ca^{2+}-induced Ca^{2+} release store was depleted by caffeine after

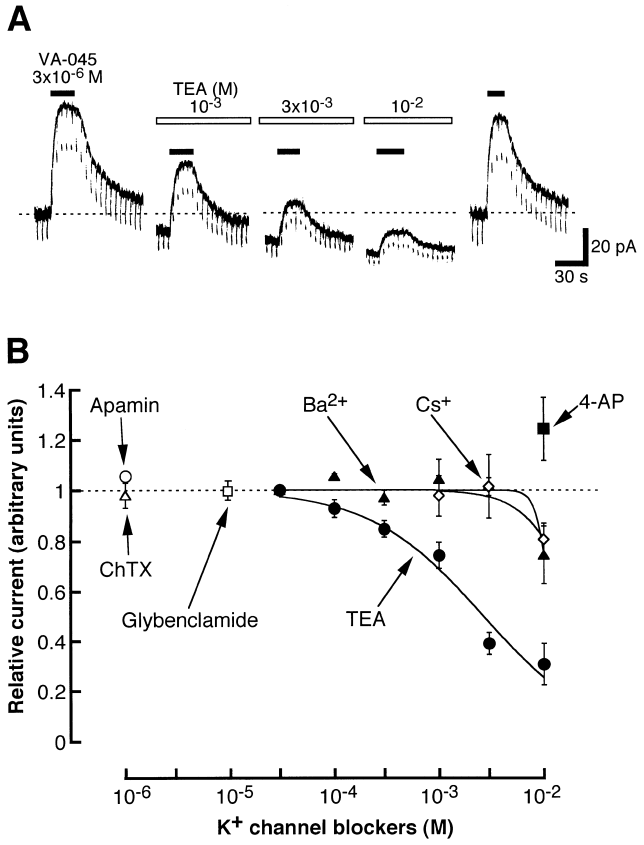

Fig. 5. The effect of tetraethylammonium (TEA) and various K^+ channel blockers on the VA-045 (VA) (3×10^{-6} M)-induced current at a V_H of –40 mV. A: Typical traces of TEA-induced inhibitory effects on the VA-induced current. To monitor the change in the membrane conductance, hyperpolarizing step pulses of 10 mV with duration of 300 ms every 5 s were continuously applied. B: Concentration-response curves of various K^+ channel blockers on the VA-induced current. The blockers used were apamin (opened circle), charybdotoxin (ChTX, opened triangle), glibenclamide (opened square), Ba^{2+} (filled triangles), Cs^+ (opened diamonds), 4-aminopyridine (4-AP, filled square) and TEA (filled circles). The VA-induced current in the presence of K^+ channel blockers was normalized to that before the application of each blocker. The pretreatment time for ChTX and apamin was 2 min, while that for the other blockers was 30 s.

pretreatment with ryanodine (Fig. 7Ab). The presence of thapsigargin did not affect the VA-induced current, while an outward current activated by ACh (arrow) was eliminated (Fig. 7Ac). This ACh-induced outward current is the K^+ current activated by Ca^{2+} mobilized from the inositol trisphosphate-induced Ca^{2+} release store (15, 16). Therefore, these results suggest that Ca^{2+} is not involved in the effect of VA. The VA-induced current was not changed by 0.1 μM staurosporine (n = 5). At this concentration, staurosporine suppresses several protein kinases, such as PKC and PKA. The current was not suppressed by either 10 μM quinacrine (n = 4), an arachidonic acid metabolism blocker, or 1 μM wortmanin (n = 5), which inhibits myosin light chain kinase. In addition, a tyrosine kinase inhibitor, 10 μM genistein (n = 4), also failed to block the current. The involvement of G protein was also assessed. The neurons were perfused with a patch pipette solution containing GTP (0.4 mM) or GDPβS (0.4 mM) in the conventional patch recording configuration. In these conditions, 3 μM VA was repeatedly applied at 2-min intervals, beginning 2 min after rupture of the membrane. Current amplitudes were normalized to the current induced by the first application of VA. Figure 7C summarizes the change in the VA-induced current amplitude 10 min after rupture of the membrane. Regardless of GDPβS, the VA-induced current gradually decreased and no significant difference was observed between these cases (n = 5). Combined, these facts indicate that second messenger systems are not involved in the effect of VA, although intracellular factors may be required to maintain the activity of the K^+ channel that was affected by VA.

DISCUSSION

In this study, we investigated the effect of VA on rat neocortical neurons by using a nystatin-perforated patch recording configuration. The external application of VA elicited an outward current carried by K^+. Since various inhibitors of known second messenger systems failed to alter the effect of VA, VA may act directly on the K^+ channels.

The VA-induced K^+ current displayed distinct pharmacological properties with K^+ channel blockers. Apamin and ChTX were not effective, which ruled out the possible involvement of Ca^{2+}-activated K^+ channels. Glibenclamide, a selective blocker of the ATP-sensitive K^+ channel, also had no effect. Cs^+ and Ba^{2+} also failed to block this current. Only TEA was strongly effective. These pharmacological properties all concur with the I_K (17 – 19). Therefore, the I_K is possibly the current activated by VA.

While other known conductances were suppressed, a hyperpolarizing step command pulse evoked a slowly inactivating outward current with a decay time constant of 30.3 ± 7.1 ms at a V_H of –40 mV. The current was activated at a test potential more positive than –60 mV (Fig. 6B) and was suppressed by 10 – 20 mM TEA (data not shown). These properties of the current were also identical to those of I_K currents in neurons of the same brain area (20) and trigeminal neurons (21). Here, if I_K were independent of the VA-induced steady state current, then I_K would still be observed during the VA-response. However, the result was that I_K apparently disappeared during the maximal VA response, suggesting that the I_K is involved in the VA-induced current.

The activated I_K showed slow inactivation without VA, while such inactivation decreased as the VA-induced cur-

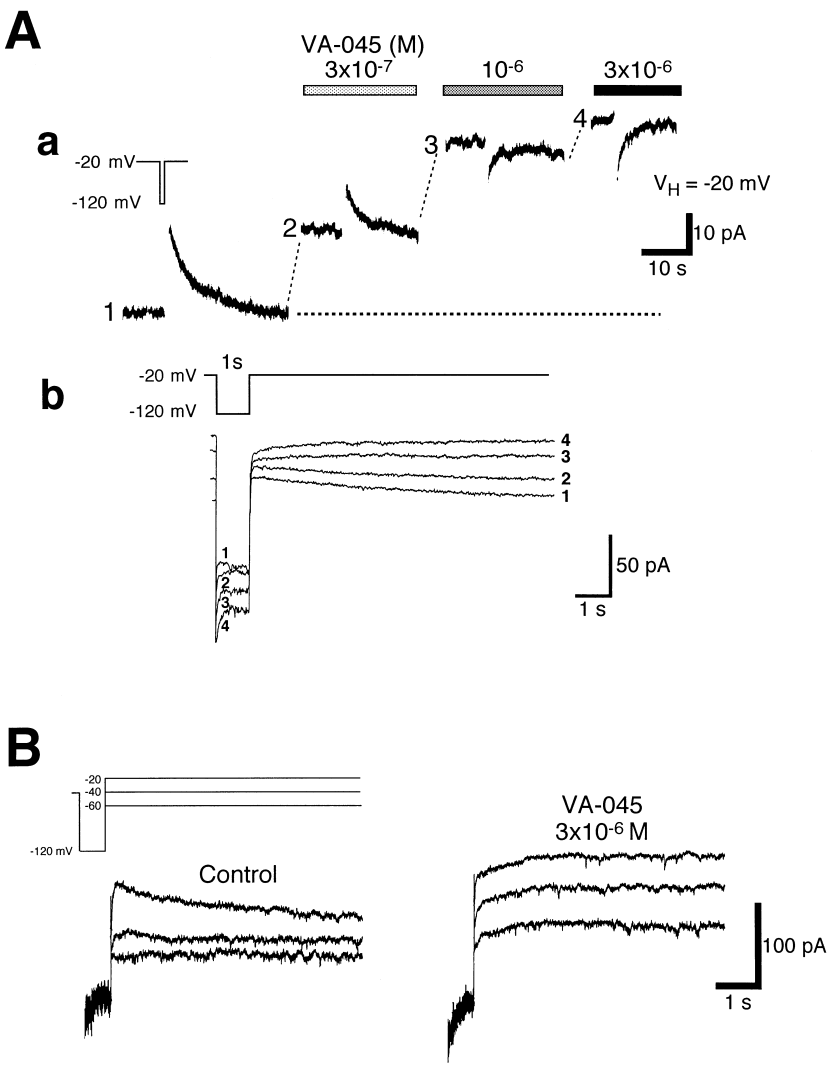

Fig. 6. The effect of VA-045 (VA) on the voltage-dependent slowly inactivating K^+ current (I_K). V_H was −20 mV. Aa: After pharmacological isolation of the I_K (see text), the I_K was evoked after a hyperpolarizing step pulse during the VA response. The current was apparently reduced during the VA-evoked outward currents. The dotted line shows the base line of current without VA under $V_H = -20$ mV. Ab: The effect of VA on the inactivation of I_K. The currents corresponding to 1 through 4 in panel Aa are drawn with a magnified time scale. As the concentration of VA increased, the inactivation of I_K was removed. B: The effect of VA on I_K evoked at various V_H's. At every V_H tested, no inactivation of I_K was observed.

rent developed (Fig. 6). Therefore, VA phenomenologically reduced the inactivation of I_K, resulting in activation of a VA-induced steady state outward current. At present, however, it is still to be elucidated whether this phenomenon resulted from removal of the inactivation state or from an extreme shift of the I_K activation or inactivation curves. Further investigation is required to clarify these points.

The I_K was not activated by a test potential more negative than −60 mV. However, the VA-induced current was observed even at a membrane potential of −100 mV. In addition, VA increased the steady state level of deactivation (Fig. 6Ab) during the hyperpolarizing steps. The threshold of activation for I_K might shift to be more negative than −100 mV or VA may affect another kind of K^+ channel.

Various ionic channels, including I_K, are modulated by multiple second messenger systems (22). Thus, we investigated whether known second messenger systems were involved in the VA-response. In our study, VA repeatedly activated outward currents in the Ca^{2+}-free external solution, even after the intracellular Ca^{2+} stores were depleted, suggesting that Ca^{2+} was not involved in the effect of VA (Fig. 7A). The VA-induced current was not changed by 0.1 μM staurosporine, which suppresses multiple protein kinases (Fig. 7B). Neither quinacrine, an arachidonic acid metabolism blocker, nor wortmanin, which inhibits myosin light chain kinase, suppressed the current (Fig. 7B). The

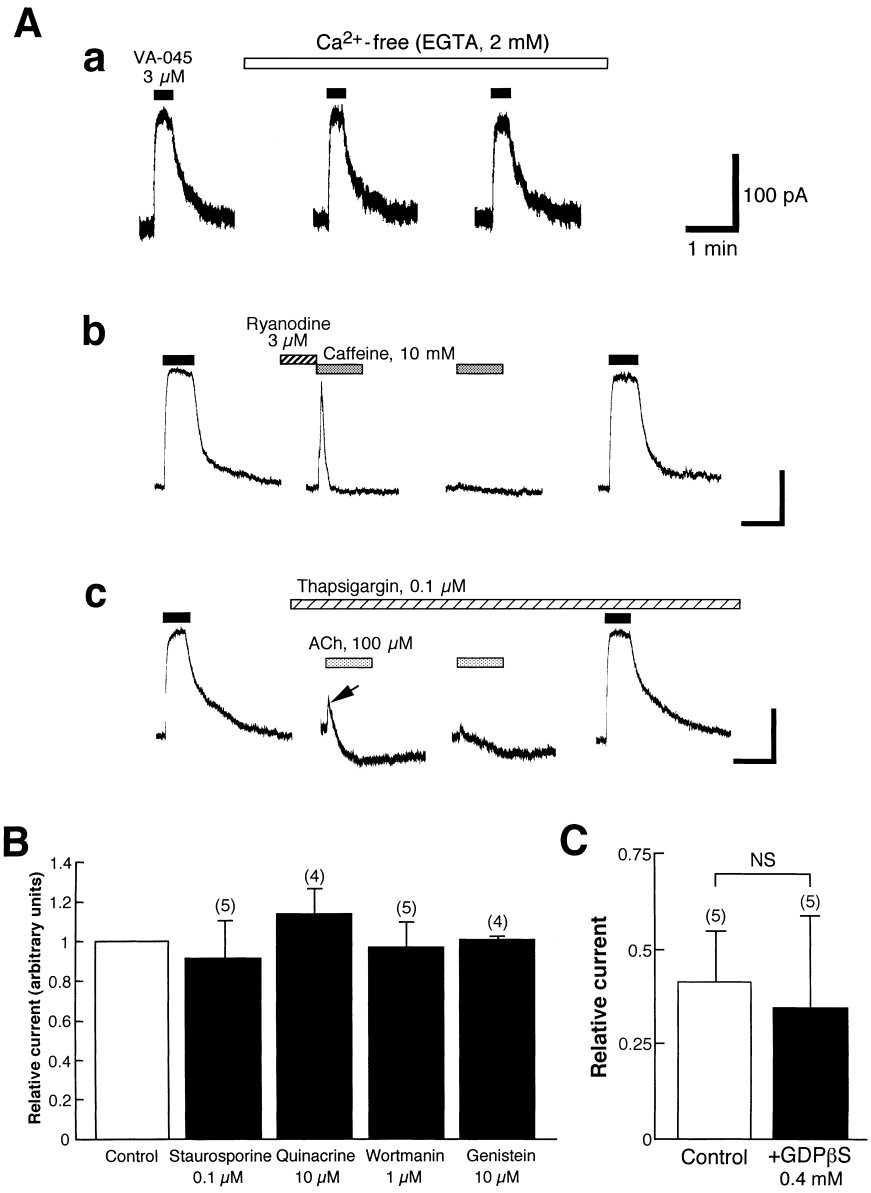

Fig. 7. The effect of blocking of the intracellular signal transduction systems on the effect of VA-045 (VA). Aa: VA repetitively elicited a at 2-min interval response, even when the external solution did not contain Ca^{2+}. Ab: The VA-induced current did not change, even when the Ca^{2+}-induced Ca^{2+} release store was depleted by caffeine and ryanodine. Ac: The effect of VA also remained after the inositol trisphosphate-induced Ca^{2+} release was depleted by ACh in the presence of thapsigargin. Caffeine and ACh were repeatedly applied at about 5-min interval, beginning >10 min after nystatin-perforated patch recording. B: Staurosporine, quinacrine, wortmanin and genistein had no effect on the VA-induced current. C: Internal perfusion of GDPβS failed to block the effect of VA. Each bar represents the mean ± S.E.M. and ( ) represents the number of neurons.

tyrosine kinase inhibitor genistein was also ineffective (Fig. 7B). In the experiment using conventional whole-cell recording, the current amplitude of the VA response gradually decreased, even in the control internal solution containing ATP. However, rundown of the VA response was not different from it with the intracellular perfusion of GTPβS (Fig. 7C). Combining these facts, VA may directly activate the channel structure.

This study revealed that VA activated a distinct K^+ current, presumably I_K. As shown in Fig. 2Aa, the increase of K^+ conductance caused by VA hyperpolarizes the membrane potential. This effect may inhibit neuronal overexcitation resulting from depolarization that occurs in hypoxia and injury (23), thereby raising the possibility that VA exerts neuroprotective effects. It was reported that VA ameliorates damaged brain function in a head injury model

of the rat in vivo (5). VA may have therapeutic potential for improving brain damage. On the other hand, VA modulates the $GABA_A$-receptor kinetics (14) and selectively dilates the cerebral artery (24). Further investigation in vivo is required to clarify what behavioral effects these basic cellular effects produce.

Acknowledgments

The authors thank Drs. Young-Ho Jin, and M. Fujimoto for their technical assistance.

REFERENCES

1 Halliwell JV: K^+ channels in the central nervous system. *In* Potassium Channels: Structure, Classification, Function and Therapeutic Potential, Edited by Cook NS, pp 348 – 381, Ellis Horwood, New York (1990)
2 Oxford GS and Wagoner PK: The inactivating K^+ current in GH3 pituitary cells and its modification by chemical reagents. J Physiol (Lond) **410**, 587 – 612 (1989)
3 Rouzaire-Dubois B and Dubois JM: Modification of electrophysiological and pharmacological properties of K channels in neuroblastoma cells induced by the oxidant chloramine-T. Pflugers Arch **416**, 393 – 397 (1990)
4 Kawashima Y, Ikemoto T, Horiguchi A, Hayashi M, Matsumoto K, Kawarasaki K, Yamazaki R, Okuyama S and Hatayama K: Synthesis and pharmacological evaluation of (nitrooxy) alkyl apovincaminates. J Med Chem **36**, 815 – 819 (1993)
5 Okuyama S, Imagawa Y, Ogawa S, Araki H, Otomo S, Sakagawa T, Yamada S and Shima K: Effect of VA-045 on a closed head injury model in rats. Life Sci **53**, 273 – 278 (1993)
6 Yamada S, Yamaguchi K and Okuyama S: Cerebral protective effects of VA-045, a novel apovincaminic acid derivative, in mice. Res Commun Mol Pathol Pharmacol **86**, 83 – 91 (1994)
7 Nishikawa M, Munakata M and Akaike N: Muscarinic acetylcholine response in pyramidal neurones of rat cerebral cortex. Br J Pharmacol **112**, 1160 – 1166 (1994)
8 Horn R and Marty A: Muscarinic activation of ionic currents measured by a new whole-cell recording method. J Gen Physiol **92**, 145 – 159 (1988)
9 Akaike N and Harata N: Nystatin perforated patch recording and its applications to analyses of intracellular mechanisms. Jpn J Physiol **44**, 433 – 473 (1994)
10 Akaike N, Lee KS and Brown AM: The calcium current of *Helix* neuron. J Gen Physiol **71**, 509 – 531 (1978)
11 Hamill OP, Marty A, Neher E, Sakmann B and Sigworth FJ: Improved patch-clamp techniques for high-resolution current recording from cells and cell-free membrane patches. Pflugers Arch **391**, 85 – 100 (1981)
12 Murase K, Ryu PD and Randic M: Excitatory and inhibitory amino acids and peptide-induced responses in acutely isolated rat spinal dorsal horn neurons. Neurosci Lett **103**, 56 – 63 (1989)
13 Akaike N, Inomata N and Tokutomi N: Contribution of chloride shifts to the fade of γ-aminobutyric acid-gated currents in frog dorsal root ganglion cells. J Physiol (Lond) **391**, 219 – 234 (1987)
14 Munakata M, Fujimoto M, Akaike N and Araki H: Nitrooxy alkyl apovincaminate modulates $GABA_A$ receptor in rat neocortical neurones. Neuroreport **7**, 613 – 616 (1996)
15 Fukuda K, Higashida H, Kubo T, Maeda A, Akiba I, Bujo H, Mishina, M and Numa S: Selective coupling with K^+ currents of muscarinic acetylcholine receptor subtypes in NG108-15 cells. Nature **335**, 355 – 358 (1988)
16 Wakamori M, Hidaka H and Akaike N: Hyperpolarizing muscarinic responses of freshly dissociated rat hippocampal CA1 neurones. J Physiol (Lond) **463**, 585 – 604 (1993)
17 Armstrong CM and Hille B: The inner quaternary ammonium ion receptor in potassium channels of the node of Ranvier. J Gen Physiol **59**, 388 – 400 (1972)
18 Adams PR, Brown DA and Constanti A: M-currents and other potassium currents in bullfrog sympathetic neurones. J Physiol (Lond) **330**, 537 – 572 (1982)
19 Tokimasa T, Tsurusaki M and Akasu T: Slowly inactivating potassium current in cultured bull-frog primary afferent and sympathetic neurones. J Physiol (Lond) **435**, 585 – 604 (1991)
20 Zona C, Pirrone G, Avoli M and Dichter M: Delayed and fast transient potassium currents in rat neocortical neurons in cell culture. Neurosci Lett **94**, 285 – 290 (1988)
21 Kitakoga O and Kuba K: Bradykinin-induced ion currents in cultured rat trigeminal ganglion cells. Neurosci Res **16**, 79 – 93 (1993)
22 Hille B: Ionic Channels in Excitable Membranes. Sinauer Associates, Sunderland, MA (1992)
23 Shimoji K, Higashi H, Fujiwara N, Fukada S and Yoshimura M: Hypoxia in brain slices. Biomed Biochim Acta **48**, S149 – S154 (1989)
24 Miyata N, Yamaura H, Tanaka M, Muramatsu M, Tsuchida K, Okuyama S and Otomo S: Effects of VA-045, a novel apovincaminic acid derivative, on isolated blood vessels: cerebroarterial selectivity. Life Sci **52**, 181 – 186 (1993)